Uncertainty Evaluation of a Supercapacitor Equivalent Circuit Parameters

Uncertainty Evaluation of a Supercapacitor Equivalent Circuit Parameters

Mauro Zucca, *Senior Member, IEEE*, Melika Hassanzadeh, Davide Signorino, and Umberto Pogliano

***Abstract*— The accurate simulation of the behavior of a supercapacitor (SC) and its control in an electronic system cannot be achieved by a simple one-branch circuit. A correct simulation requires the use of more complex equivalent circuits, with at least two or three branches. These equivalent circuits guarantee a good reproduction of the device's behavior. The effectiveness of an equivalent circuit is linked to the limits of the circuit parameter identification, which is commonly achieved by means of the voltage and current measurement of charge and self-discharge cycles. The uncertainty in the identification of these circuit parameters is dependent on the accuracy of the measurement instrumentation and on the repeatability of the SC. A cycle for determining the parameters can extend over a few hours for larger SCs, also considering the time needed by the software algorithm for the parameter identification. Therefore, having a large set of cycles including the determination of the parameters is a time-consuming procedure. In this study, an efficient method for the repeatability and uncertainty assessment of the equivalent circuit parameters is proposed; this approach relies on a limited set of experimental data and on a single parameter identification process. The analysis presented in this article highlights how the limited repeatability of the device is an important source of uncertainty for the identification of the equivalent circuit parameters, but it is not the main one for all parameters.**

***Index Terms*— Least-squares approximations, mathematical models, measurement, parameter estimation, supercapacitors (SCs), uncertainty.**

I. Introduction

THE availability of supercapacitor (SC) equivalent circuits is useful for several reasons: it allows the correlation of circuit parameters with other quantities, such as the state of charge (SoC) or state of health (SoH), and allows the modeling of SCs in complex electronic circuits. This approach for SC characterization that occurs in the time domain is not the only possible one; other approaches based on techniques in the frequency domain, such as electrochemical impedance spectroscopy (EIS), can provide equally useful parameters for the determination of SC behavior and correlation with SoC and SoH.

Currently, state-of-the-art techniques do not provide a leading technique for the characterization of SCs, and all adopted techniques have intrinsic limitations. For example, EIS implies a linearization of the behavior of the SC (which by its nature is nonlinear); to date, EIS has no traceability for capacitances above one farad, even if strong efforts are being made in this direction [1], [2], [3], [4], [5]. However, the determination of the equivalent circuit relies on traceable measurements of the current and voltage, but it can be more time-consuming and does not provide immediate frequency behavior. Both techniques depend on the repeatability of the device.

This study focuses on time-domain techniques for the determination of capacitance parameters, electrical series resistance (ESR), and other equivalent circuit parameters, especially because time-domain measurement techniques are considered by international reference standards [6], [7].

The identification of an equivalent circuit through measurements is not a trivial process and a wide number of papers have been published in the literature [8], [9], [10], [11], [12], [13], [14]. However, to the best knowledge of the authors, there are not many references describing the evaluation of uncertainty in the determination of parameters, including repeatability. Most studies have discussed the ability of a model to reproduce an SC voltage terminal.

The novelty of this study is the proposal of an effective and general method for evaluating the uncertainty in the determination of circuit parameters, which has been validated for two-branch or three-branch models [15]. This is done by extending the conference paper [16] dealing with repeatability.

This article is organized as follows. Section II briefly describes the modeling approach. Section III highlights how the same relative variations of each circuit parameter have a different effect on the voltage at the SC terminals. Section IV discusses the uncertainty term due to the repeatability of the measurements. Finally, Section V discusses the uncertainty terms obtained from the measurements, which are necessary for identification, and an overall assessment of the uncertainty in the estimation of the circuit parameters is carried out.

II. Modeling

Four families of models are available for simulating the behavior of SCs: 1) electrochemical models [17]; 2) fractional-

Received 4 November 2024; revised 3 January 2025; accepted 17 January 2025. Date of publication 21 February 2025; date of current version 19 March 2025. This work was supported by the European Union through the Horizon Europe Research and Innovation Programme, within the framework of the EMPHASIS Project under Grant 101091997 and the 23IND04 MetSuperCap Project. This latter has received funding from European Partnership on Metrology, co-financed from the Horizon Europe programme and by the Participating States. The Associate Editor coordinating the review process was Dr. Qing Wang. *(All authors contributed equally to this article.) (Corresponding author: Mauro Zucca.)*

Mauro Zucca, Davide Signorino, and Umberto Pogliano are with the Istituto Nazionale di Ricerca Metrologica (INRiM), 10135 Turin, Italy (e-mail: m.zucca@inrim.it; d.signorino@inrim.it; u.pogliano@inrim.it).

Melika Hassanzadeh is with the Istituto Nazionale di Ricerca Metrologica (INRiM), 10135 Turin, Italy, and also with the DISAT, Politecnico di Torino, 10129 Turin, Italy (e-mail: mailto:melika.hassanzadeh@polito.it).

Digital Object Identifier 10.1109/TIM.2025.3544362

order models [18], [19], [20], [21], [22]; 3) equivalent circuit models (ECMs) [23], [24], [25], [26], [27], [28]; and 4) machine-learning-based models, often combined with one of the previous models [29].

This study deals with ECMs, focusing on two- and three-branch models. A discussion of the existing circuit models in the literature is also reported in [15].

A. Equivalent Circuit Identification

Regardless of the modeling approach, the identification of an equivalent circuit in the time domain is obtained by dynamic driving cycles [13] charge and discharge (or self-discharge) cycles, with or without the integration of EIS measurements [24], [28]. The temperature effect is often considered [14], but the repeatability effect is generally disregarded, even if in some papers, measurement noise is introduced as an identification parameter (e.g., [24]).

It should be noted that discharge and self-discharge are two different phenomena. The discharge of an SC occurs when a load current is applied to the SC, which can be easily simulated by a two-quadrant generator. In this case, a discharge occurs, which is normally controlled at a constant current. Self-discharge occurs when no load is applied to the capacitor; therefore, the device does not supply any current. The self-discharge appears due to internal mechanisms within the SC that cause leakage of charge (internal leakage currents, surface and interface effects in the dielectric, and so on), resulting in a reduction of the stored voltage and energy.

In this study, the temperature effect is neglected, and identification is considered at a constant temperature; however, the repeatability effect is specifically considered in the second part of the identification process. The circuit model is identified through a charge and self-discharge cycle. In the charging phase, a time constant that governs the charge up to the nominal voltage can be identified. When the rated voltage is reached, the current is suddenly set to zero in a few tens of milliseconds at maximum. The current goes to zero and the voltage drop on the series resistance (R_i) is also subtracted from the terminal voltage, which is the vertical drop in Fig. 1. From that moment, at the end of the vertical drop, the self-discharge phase begins and it is possible to identify at least a second-time constant. Depending on the considered time window and size of the SCs, a third-time constant can be identified.

Fig. 1 shows three charge and self-discharge cycles for three SCs: 100 F with a nominal voltage of 3 V and charged with a constant current of 10 A, 400 F with a nominal voltage of 2.7 V and charged with a constant current of 20 A, and 1500 F with a nominal voltage of 2.7 V and charged with a constant current of 50 A. The diagram shows the normalized terminal voltage as a function of time. The three capacitors are charged at a constant current until they reach the nominal voltage and the current stops; at the same time, a voltage drop occurs, which provides the typical "tooth" to the curve; then, the self-discharge begins.

It is interesting to compare the self-discharge curve of the 1500-F SC and that of the 100-F SC. As highlighted in the inset, after the peak, the green curve clearly shows two different slope areas (double time constants), whereas the blue curve can be approximated by a curve with a single time constant. In other words, the small 100-F capacitor, as well as the 400-F one, can be simulated using a three-branch circuit, while the 1500-F capacitor can be simulated using a two-branch circuit. The type and value of the equivalent circuit parameters also depend on the chosen time window. For this study, we limited the identification of an equivalent circuit with a self-discharge time window of no longer than 2 h.

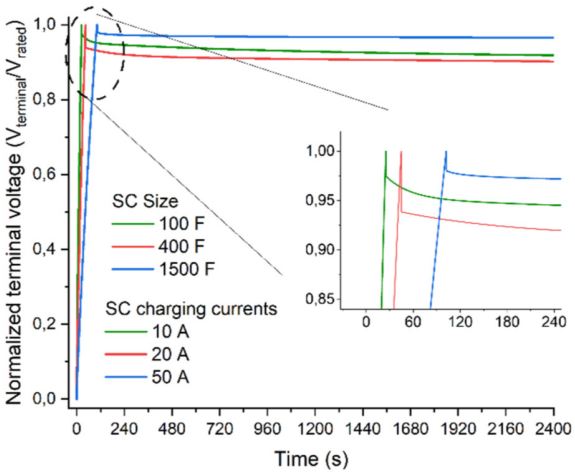

Fig. 1. Normalized charge and self-discharge terminal voltage for the different SCs: 100 F (rated voltage 3 V), 400 F (rated voltage 2.7 V), and 1500 F (rated voltage 2.7 V). Charge is performed at constant current.

B. Mathematical Model

Modeling in this study refers to two-branch or three-branch models. The identification is performed by including the model in a procedure that minimizes the difference between the measured terminal voltages in a charge and self-discharge cycle and the simulation results. The procedure is described in detail in [15] and the main steps are described as follows.

The state equation vector can be obtained with reference to the circuit shown in Fig. 2 as follows:

$$\dot{\boldsymbol{v}} = \boldsymbol{A}\boldsymbol{v} + \boldsymbol{B}y \tag{1}$$

where $\boldsymbol{v}$ is the vector representing the state variables, which are the capacitor voltages (2); and $\dot{\boldsymbol{v}}$ is the time-derivative vector (3). $\boldsymbol{A}$ (4) is the state matrix; $\boldsymbol{B}$ (5) in linear systems is the so-called input vector; and y is the input equal to the difference between the imposed and the leakage currents, which is a scalar function in this case: $y = i - i_{\text{lea}}$, the leakage resistance being known

$$\boldsymbol{v} = \begin{bmatrix} V_i \\ V_d \\ V_l \end{bmatrix} \tag{2}$$

$$\dot{\boldsymbol{v}} = \begin{bmatrix} \dfrac{dV_i}{dt} \\ \dfrac{dV_d}{dt} \\ \dfrac{dV_l}{dt} \end{bmatrix} \tag{3}$$

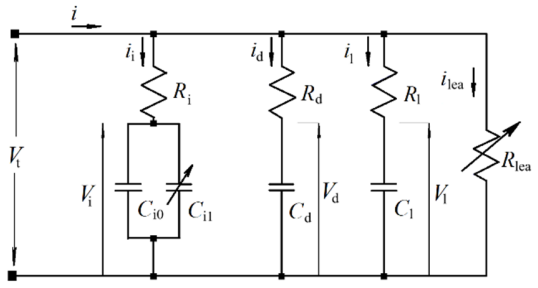

Fig. 2. Three-branch equivalent circuit proposed in [15].

$$\boldsymbol{A} = \begin{bmatrix} \frac{-(R_d + R_l)}{\text{den} \cdot C_i(V_i)} & \frac{R_l}{\text{den} \cdot C_i(V_i)} & \frac{R_d}{\text{den} \cdot C_i(V_i)} \\ \frac{R_l}{\text{den} \cdot C_d} & \frac{-(R_l + R_i)}{\text{den} \cdot C_d} & \frac{R_i}{\text{den} \cdot C_d} \\ \frac{R_d}{\text{den} \cdot C_l} & \frac{R_i}{\text{den} \cdot C_l} & \frac{-(R_i + R_d)}{\text{den} \cdot C_l} \end{bmatrix} \tag{4}$$

$$\boldsymbol{B} = \begin{bmatrix} \frac{R_d R_l}{\text{den} \cdot C_i(V_i)} \\ \frac{R_l R_i}{\text{den} \cdot C_d} \\ \frac{R_i R_d}{\text{den} \cdot C_l} \end{bmatrix} \tag{5}$$

where

$$\text{den} = R_i \cdot R_l + R_i \cdot R_d + R_d \cdot R_l. \tag{6}$$

Equation (1) is nonlinear because the matrix of coefficient $\boldsymbol{A}$, the input vector $\boldsymbol{B}$, and the leakage current depend all on V_i.

The efficient nonlinear minimization procedure applied to this problem is the conventional trust region reflection (CTRR) method [30], [31]. In [15], it is reported schematically how the optimization is implemented for the identification, through minimization, of the circuit parameters, starting from the initial trial values. The only parameter that is defined offline is the leakage resistance R_{lea} [15], which determines the leakage current i_{lea}.

The solution of the two-branch problem is obtained in the same way. In this case, a very large value of R_l ($\geq$100 MΩ) is imposed so that the third branch is inactive.

C. Measurement Method

The present study utilizes current and voltage measurements on an SC to identify and verify the proposed models. The current measurement is performed using an LEM IT_65-S Ultrastab transducer, with an expanded uncertainty limited to 0.1 ‰ in dc. Two channels of a National Instruments PCI eXtensions for Instrumentation (PXI)-4461 board fit with a delta–sigma analog-to-digital converter at 24 bits were used as digitizers. The voltage is measured directly on one channel of the board with a voltage range of $\pm$3.16 V. Measurements are acquired and managed using a program created in the LabVIEW environment. To provide constant charging and discharging currents, an ITECH IT-6015-C bidirectional programmable dc power supply is used in the experimental setup. All measurements and investigations were performed in a temperature-controlled room (23 °C $\pm$ 0.5 °C). The devices under test (DUT) are three electric double-layer capacitors (EDLCs): the first, is a 100-F SC (Eaton TV1860-3R0107-R), the second a 400-F SC (Eaton XV series), the same utilized in [16] and similar to the one (but not the same) utilized in [15], and the third a 1500-F SC (SPSCAP SCP1500C0-0002R7STA). The following results are obtained at constant charging currents of 10, 20, and 50 A, for the three SCs.

III. Quantities of Interest

The dynamics of the circuit should not be new to the readers. In summary, the resistance R_i and capacitances C_{i0} and C_{i1}, which are components of a linear approximation of $C_i(V_i)$, define the charging behavior of the SC. C_d and R_d define the first time constant during self-discharge (faster discharge phase), whereas R_l and C_l define the time constant of the longer self-discharge phase. The leakage resistance (R_{lea}) is considered as a constant in this analysis because discharges longer than 2 h are not considered in this study. A discussion of long discharging times and about the determination of R_{lea} can be found in [15].

The variation in these parameters has a different effect on the terminal voltage in terms of the amplitude and time span.

An estimation of the parameter variation effect can be obtained by sensitivity analysis, which is not limited to the three-branch model analyzed here.

In the n-branch SC model, the voltage at the terminals can be expressed as

$$u(t) = f(P_1, P_2, \ldots, P_k, i(t)) \tag{7}$$

where $u(t)$ is the time behavior of the voltage at the terminals, $i(t)$ is the time behavior of the current, and $P_1, \ldots, P_k$ are the generic parameters that here are the circuital parameters in Fig. 2.

If a specific function of the measured current $i_m(t)$ is considered, the sensitivities of the output $u(t)$ can be analytically or numerically evaluated as a function of every parameter as

$$S_{P_j}(i_m(t), t) = \frac{\partial u(t)}{\partial P_j} = \frac{\partial f(P_1, P_2, \ldots, P_k, i_m(t))}{\partial P_j}. \tag{8}$$

In a discrete approach, by imposing a parameter variation $\Delta P_j = \alpha_j P_j$, where $-0.1 \leq \alpha_j \leq 0.1$, the sensitivity can be expressed as

$$S_{P_j}(i_m(t), t) = \frac{\Delta u(t)}{\Delta P_j} = \frac{\Delta u(t)|_{\alpha_j P_j}}{\alpha_j P_j} \tag{9}$$

where $S_{P_j}(i_m(t), t)$ is the absolute sensitivity owing to the absolute parameter variation. The sensitivity to the relative change of parameter P_j can be written as

$$S_{R,P_j}(i_m(t), t) = \frac{\Delta u(t)|_{\alpha_j P_j}}{\frac{\alpha_j P_j}{P_j}}. \tag{10}$$

Immediate comparability among different parameters is the main advantage of the sensitivity to the relative change of parameter P_j (10).

Because the behavior of an SC is nonlinear, the sensitivity analysis also shows nonlinearity, although to a limited extent.

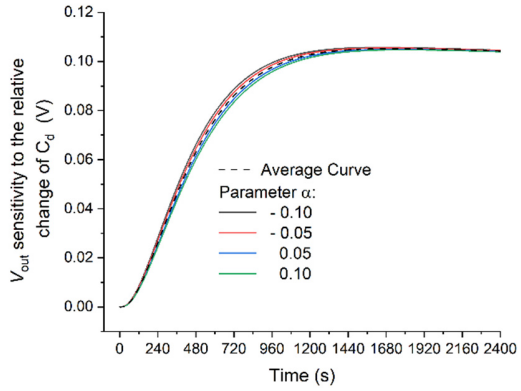

Fig. 3. Computed time behavior of the sensitivity of relative change of the parameter C_d for 400-F SC.

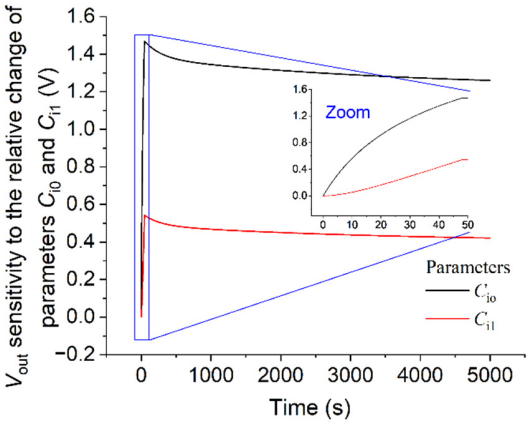

Fig. 4. Computed time behavior of the sensitivity to the relative change of parameters C_{i0} and C_{i1} (400-F SC).

Fig. 3 shows the sensitivity related to the parameter C_d for imposed variations of the parameter equal to $\pm 5\%$ and $\pm 10\%$. As can be seen, the curve has a slight drift when changing the parameter variation from -10% to $+10\%$. In the following, the average sensitivity curve, which is highlighted in the same diagram for C_d, is referenced without losing analysis generality.

Figs. 4 and 5 compare the relative sensitivities of all the parameters. As S_R of C_{i0} and C_{i1} is approximately one order of magnitude higher than that of the others, it has been reported in a separate diagram (see Fig. 4).

S_R of the leakage resistance is nearly negligible, less than 0.012 V, and has not been reported because this parameter is determined "offline" using a separate method [15].

It can be noted that S_R of the resistance parameters has the opposite sign to that of the capacitances, which allows the equivalent circuit to obtain excellent measurement fitting.

Table I lists the maximum sensitivity values and normalized percentage values to the relative change of various parameters. These values will be useful in the discussion in Section IV.

IV. Limited Repeatability of the Measurements

Repeatability is an important parameter mentioned in the standards that underlines how SCs need training before

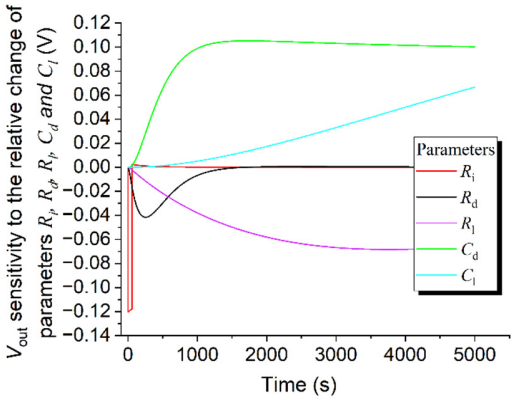

Fig. 5. Computed time behavior of the sensitivity to the relative change of parameters R_i, R_d, R_l, C_d, and C_l (400-F SC).

TABLE I
Sensitivity to the Relative Change of the Seven Circuital Parameters for 400-F SC

	C_{i0}	C_{i1}	C_d	C_l	R_i	R_d	R_l
$\lvert S_{R\_max}\rvert$(V)	1.470	0.543	0.105	0.067	0.120	0.041	0.068
Norm. $\lvert S_{R\_max}\rvert$%	100	36.9	7.1	4.6	8.1	2.8	4.6

parameter measurements and assessments. For example, in [7], all measurement test descriptions state that "charging and discharging can be repeated, if necessary until the capacity and internal resistance are stabilized," highlighting the problem but without going into details about its quantification.

A. Approach to Repeatability Assessment

In this work, we observed that effective training is as follows. A charging phase is maintained for half an hour at the rated voltage, followed by a self-discharge of 2 h, and a subsequent complete discharge imposing a negative current. This cycle is followed by a simple charge and self-discharge cycle. After approximately ten complete cycles, the charge and self-discharge cycle repeatability becomes acceptable even for larger, new SCs or SCs subjected to long standby phases. Fig. 6 shows the training of the 1500-F SPS-CAP SC whose training was recorded from its state "just purchased, new." Its training performance is typical and similar to that of the other two SCs. Fig. 6(a) shows the first six cycles performed on an SC on the first day, whereas Fig. 6(b) shows the same number of cycles performed the following day. At this point, a reasonable repeatability is achieved, which is maintained even after several days. Fig. 6(c) and (d) shows the cycles repeated five and six days after the previous cycles. Fig. 6(e) shows in full scale the set of all the cycles of all the days, while Fig. 6(f) shows in full scale all the cycles, except for the first ten cycles. The last figure represents the cycles suitable for the study of repeatability and that of the training should be discarded.

As shown in [16], there is better repeatability in the charging phase than in the self-discharge phase. Because the cycles do not perfectly overlap, this implies a certain variability in the

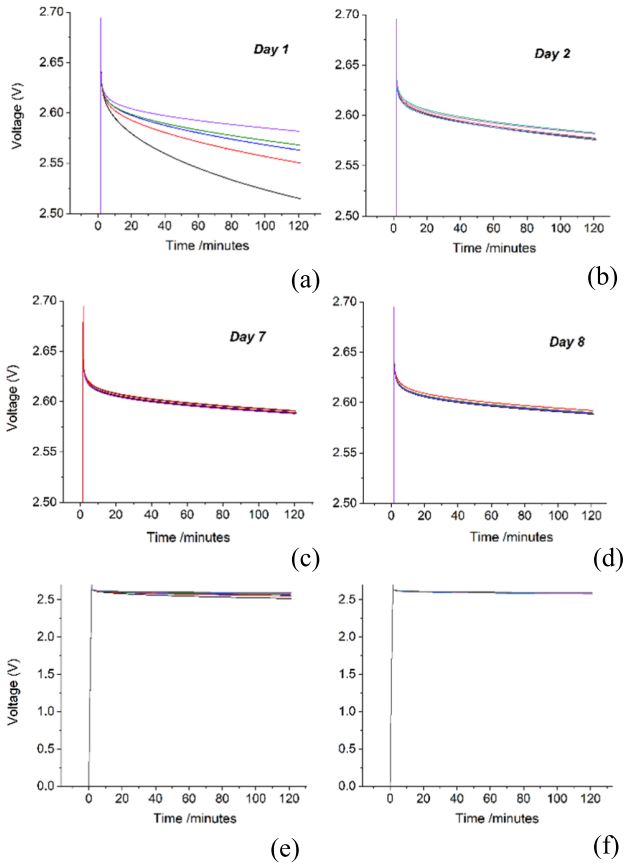

Fig. 6. Charge and self-discharge diagrams for an SC 1500 F (SPSCAP SCP1500C0-0002R7STA). (a)–(d) Repeated and measured on different days. (e) Overall full-scale diagram of all cycles. (f) Diagram of all cycles except the first 10.

circuit parameters. To evaluate such variability, it is necessary to have a large group of charging and self-discharging curves, where the equivalent circuit parameters are identified for each. Because this process is time-consuming, once the training is performed, it is sufficient to record a number of curves greater than or equal to the circuit unknowns, which are seven in the considered model. Generally, ten or 12 curves are sufficient for an overdetermined system to assess the parameter variability.

As discussed in the next paragraph, by applying the proposed method, it is possible to reconstruct the parameter variability starting from a single identification procedure.

B. Method to Speedup the Repeatability Assessment

Starting from a set of charge and self-discharge cycles, with at least $(m+1)$ measured behaviors of the current and voltage $i_m(t)$ and $u_m(t)$ at the SC terminals, where $m > k$ and k is the number of electrical parameters, one can choose a specific measurement as a reference, for example, the one closest to the mean behavior. For every measurement set, we define the voltage-difference function as follows:

$$\Delta u_j(t) = u_j(t) - u_{\text{ref}}(t).$$

Considering n time samples $t_1, t_2, \ldots, t_n$ for every measurement set, expressing the set of variations in matrix form, we obtain

$$\begin{bmatrix} \Delta u_1(t_1) & \ldots & \Delta u_m(t_1) \\ \ldots & \ldots & \ldots \\ \Delta u_1(t_n) & \ldots & \Delta u_m(t_n) \end{bmatrix} = \begin{bmatrix} S_{P_1}(i_m(t_1), t_1) & \ldots & S_{P_k}(i_m(t_1), t_1) \\ \ldots & \ldots & \ldots \\ S_{P_1}(i_m(t_n), t_n) & \ldots & S_{P_k}(i_m(t_n), t_n) \end{bmatrix} \times \begin{bmatrix} \Delta P_{11} & \ldots & \Delta P_{1m} \\ \ldots & \ldots & \ldots \\ \Delta P_{k1} & \ldots & \Delta P_{km} \end{bmatrix} \tag{11}$$

that is,

$$\Delta \mathbf{U} = \mathbf{S_P} \cdot \Delta \mathbf{P} \tag{12}$$

where $\Delta \mathbf{U}$ is the matrix containing the voltage-difference functions in the columns; $\mathbf{S_P}$ is the sensitivity matrix; and $\Delta \mathbf{P}$ is the parameter variation for every measurement set, which is unknown in this investigation.

The optimal circuit parameters can be estimated only for the reference curve (single measurement) according to [15]. The sensitivity parameters can be computed by the equivalent circuit of the reference curve, imposing a parameter variation ΔP and checking the voltage terminal variation Δu. The distribution of the parameters around the optimal ones can be computed by repeating the voltage measurements as follows:

$$\Delta u(t) = S_{P_1}(i_m(t), t) \cdot \Delta P_1 + \cdots + S_{P_k}(i_m(t), t) \cdot \Delta P_k. \tag{13}$$

By applying the least-squares principle [32], we can derive the parameter variations for the set of measurements as follows:

$$\Delta \mathbf{P} = \left(\mathbf{S_P^T} \cdot \mathbf{S_P}\right)^{-1} \cdot \mathbf{S_P^T} \cdot \Delta \mathbf{U}. \tag{14}$$

Here, for a specific test current, the sensitivities and matrix $(\mathbf{S_P^T} \cdot \mathbf{S_P})^{-1} \cdot \mathbf{S_P^T}$ are computed only once.

Table II presents the analysis of the parameter variability for the three considered SCs. Equation (14) provides a variability vector for each parameter whose distribution, as shown in Fig. 7, for the parameters R_d and C_d, tends toward a Gaussian distribution. The average parameter variability, ΔP_{avg} is presented in Table II. The percentage parameter variation (PPV) defined as

$$\text{PPV} = \frac{2\sigma_{P\_\text{rea}}}{P_0 + \Delta P_{\text{avg}}} \cdot 100 \tag{15}$$

is computed as a function of ΔP_{avg} and σ_{P_rea}, where σ_{P_rea} is the standard deviation owing to repeatability. PPV and σ_{rea} are included in Table III.

C. Discussion on Repeatability

It is interesting to compare the results in Table II with Table I and Figs. 4 and 5. The parameter C_{i0}, which shows the highest $S_{R\text{max}}$ at the terminal voltage, has the lowest PPV variation. The parameter C_{i1}, which has $S_{R\text{max}}$ about one-third of C_{i0}, has a PPV of about three times. The other parameters, which have $S_{R\text{max}}$ less than one-tenth of that of C_{i0}, have a PPV that is about an order of magnitude higher. In general,

TABLE II
PARAMETERS AND VARIATIONS FOR 100-/400-/1500-F SCs

Param.	Param. Value P_0	Averaged variation ΔP_{avg}	Standard deviation σ_{P_rea}	Param. Percent. variation PPV / %
100 F				
R_i (mΩ)	7.46	-0.38	0.25	7.06
C_{i0} (F)	48.5	0.38	0.24	0.98
C_{i1} (F)	12.18	0.02	0.12	1.97
R_d (Ω)	6.52	0.67	0.84	23.37
C_d (F)	4.71	-0.33	0.22	10.05
R_l (Ω)	262.8	3.30	18.7	14.05
C_l (F)	3.09	0.25	0.19	11.38
400 F				
R_i (mΩ)	8.28	-0.069	0.062	1.51
C_{i0} (F)	260.0	-0.51	0.72	0.55
C_{i1} (F)	36.83	0.29	0.34	1.83
R_d (Ω)	11.13	0.028	0.42	7.53
C_d (F)	13.60	0.062	0.61	8.92
R_l (Ω)	249.3	-0.51	15.49	12.4
C_l (F)	12.08	0.38	1.22	19.58
1500 F				
R_i (mΩ)	1.00	-0.004	0.002	0.40
C_{i0} (F)	1352.6	-0.17	0.43	0.06
C_{i1} (F)	224.84	0.32	0.25	0.22
R_d (Ω)	42.53	0.17	0.41	1.92
C_d (F)	27.10	0.01	0.16	1.18

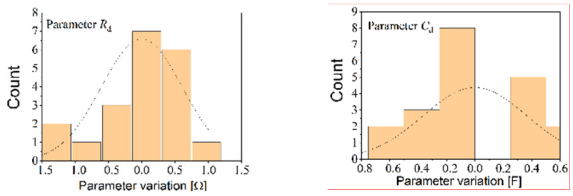

(a) (b)

Fig. 7. Frequency distribution obtained for the 400-F SC circuital parameters (a) R_d and (b) C_d, with 20 charge and self-discharge cycles.

it can therefore be stated that the parameters that show a higher PPV have a lower sensitivity, and vice versa. Table III shows how the product $|S_{R_\max}|\cdot$PPV produces results of the same order of magnitude, which means that parameters with different percentage variations owing to repeatability produce comparable maximum variations in the SC terminal voltage. This means that all the components of the equivalent circuit contribute to the definition of the terminal voltage during the charge and self-discharge process. It is also interesting to note that the variability of the parameters decreased as the SC size increased, as shown in Fig. 8.

V. UNCERTAINTY EVALUATION

To obtain the value of the overall uncertainty, it is important to emphasize that the data acquisition system and current sensor used for this application have been calibrated before being used. The calibration of PXIe 4461 was obtained for both the voltage and current channels with a Fluke 5730A calibrator with a maximum expanded uncertainty of 45 μV under static conditions, considering a rectangular distribution.

First, several amplitudes ranging from 0 to 3.6 V were generated by the calibrator and acquired by the acquisition board. Starting from the experimental data, a first-order curve fit was

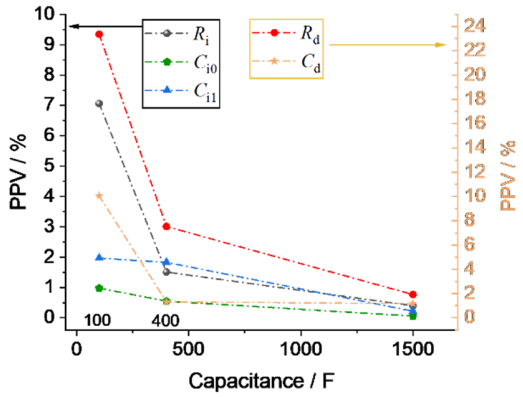

Fig. 8. Parameter percentage variation versus the SC size.

identified with an associated root-mean-square error (RMSE) lower than 200 μV. The obtained curve was adopted for systematic error compensation when performing the measurements. For each measurement point, the associated uncertainty u_{vms} was determined by considering the uncertainty of the calibration and the RMSE.

A. Uncertainty Contribution of the Measuring System

1) Current Measurement: The inaccuracies of the instrumentation used for the voltage and current measurements contributed to the uncertainty in the determination of the equivalent circuit parameters. The uncertainty due to the measurement of the current generated by the current generator can be evaluated from the uncertainty of the two currents $i_{\text{ch}}(t)$ and $i_{s\_\text{dis}}(t)$ (charge and self-discharge currents, respectively), the uncertainties of which can be considered as a first approximation, constant in both periods and uncorrelated. Because the discharge part is self-discharge, the discharge current is generated by SC internal phenomena, the generator circuit is open in this phase, and the generated current is equal to zero. The current measurement uncertainty u_{i_ch} was estimated during sensor calibration to be lower than 100 μA/A, which includes the uncertainty of the PXI acquisition card. From the variations of the charging current ΔI_{ch} set equal to the absolute variation corresponding to the measurement uncertainty, it is possible to evaluate the variations of the resulting voltage at the terminal of the SC as $\Delta\mathbf{U}_{\text{cur}}$, which is the vector of the variation of the terminal voltage at each time instant obtained from the two-branch or three-branch circuit model, by applying an excitation current variation equal to ΔI_{ch}. The variation of the parameters $\Delta\mathbf{P}_{\text{cur}}$ is obtained from the maximum current variation ΔI_{ch} as

$$\Delta\mathbf{P}_{\text{cur}} = \left|\left(\left(\mathbf{S}_P^{\text{T}}\cdot\mathbf{S}_P\right)^{-1}\cdot\mathbf{S}_P^{\text{T}}\right)^{T}\cdot\Delta\mathbf{U}_{\text{cur}}\right|. \tag{16}$$

The results of the parameter variation estimation are shown in Table IV.

2) Voltage Measurement: For the uncertainty of the voltage measuring system during the charging and self-discharging cycles, we do not know the exact behavior of the error as a function of time, which would be necessary to determine the variation in the circuit parameters. However, we only know its

TABLE III
PRODUCT $|S_{R_MAX}|\cdot$PPV

SC	R_i	C_{i0}	C_{i1}	R_d	C_d	R_l	C_l
400 F (V)	0.18	0.81	0.99	0.31	0.94	1.49	1.31

TABLE IV
OVERALL UNCERTAINTY

Param.	Average param. Value	Standard deviation due to repeatab. (Table II)	Param. max. variation due to current uncert. Eqn. (16)	Max. param. variation due to voltage uncert. Eqn. (17)	Overall expanded uncert. (k=2)
100 F	$P_0+\Delta P_{avg}$	σ_{P_rea}	ΔP_{cur}	ΔP_{vms}	U_P
R_i (mΩ)	7.08	0.25	0.01	0.04	0.50
C_{i0} (F)	48.9	0.24	0.01	0.06	0.49
C_{i1} (F)	12.2	0.12	0.02	0.03	0.24
R_d (Ω)	7.19	0.84	0.19	0.20	1.71
C_d (F)	4.38	0.22	0.02	0.05	0.44
R_l (Ω)	266.1	18.7	3.12	2.97	37.73
C_l (F)	3.34	0.19	0.02	0.12	0.41
400 F	$P_0+\Delta P_{avg}$	σ_{P_rea}	ΔP_{cur}	ΔP_{vms}	U_P
R_i (mΩ)	8.21	0.062	0.01	0.02	0.13
C_{i0} (F)	259.5	0.72	0.08	0.24	1.47
C_{i1} (F)	37.12	0.34	0.01	0.11	0.69
R_d (Ω)	11.16	0.42	0.88	0.17	1.33
C_d (F)	13.66	0.61	0.30	0.11	1.27
R_l (Ω)	248.8	15.49	8.11	16.15	37.35
C_l (F)	12.46	1.22	3.05	3.90	6.22
1500 F	$P_0+\Delta P_{avg}$	σ_{P_rea}	ΔP_{cur}	ΔP_{vms}	U_P
R_i (mΩ)	0.996	0.002	0.001	0.01	0.01
C_{i0} (F)	1352.43	0.43	0.19	0.97	1.43
C_{i1} (F)	225.16	0.25	0.03	0.36	0.65
R_d (Ω)	42.7	0.41	0.06	0.84	1.27
C_d (F)	27.11	0.16	0.04	0.35	0.52

uncertainty as a function of the voltage. Different approaches can be used to evaluate the uncertainty correctly.

1) A calculation with a statistical evaluation would require some assumptions regarding the correlation of the error at different time instants.
2) Hypothesizing a series of values related to the instrumentation error function, reported as time functions, and then evaluating the distribution of the circuit parameter variations, for repeatability (see Section IV).
3) A third possibility that certainly maximizes the effect of the error is the one considered below, which uses the maximum absolute variation of the voltage error function, after the correction of the systematic effects of the instrumentation, as a function of time (point by point).

From the maximum error at any time instant, the maximum variation of each parameter can be evaluated using the absolute values of the matrix elements

$$\Delta\mathbf{P}_{vms} = \left|\left(\left(\mathbf{S}_P^{\mathrm{T}}\cdot\mathbf{S}_P\right)^{-1}\cdot\mathbf{S}_P^{\mathrm{T}}\right)\right|\cdot|(\Delta\mathbf{u}_{\mathrm{vms}})| \qquad (17)$$

where $(\Delta\mathbf{P}_{vms})$ is the module of the maximum value of the parameter variations due to the voltage measurement system (subscript vms), and $abs(\Delta\boldsymbol{u}_{\mathrm{vms}})$ is the maximum absolute value of the voltage error due to the measurement system as a function of time.

B. Overall Uncertainty

In Table IV, we report the average parameter values for each SC as the parameter values identified with the model corrected by the average value obtained from the repeatability analysis (Table II). The overall uncertainty is also added for each SC, which includes the following contributions: 1) the repeatability standard deviation $\sigma_{P_{\mathrm{rea}}}$; 2) the parameter variation due to a maximum current variation corresponding to the current uncertainty, computed according to (16); and 3) the maximum parameter variation due to voltage uncertainty related to the measurement system $\mathbf{\Delta P}_{\mathrm{vms}}$ computed according to (17).

The overall expanded uncertainty comes from the composition of the three terms as follows:

$$U_P = k\cdot\sqrt{(\sigma_{P\_\mathrm{rea}})^2+\left(\frac{\Delta P_{\mathrm{cur}}}{\sqrt{3}}\right)^2+\left(\frac{\Delta P_{\mathrm{vms}}}{\sqrt{3}}\right)^2}. \qquad (18)$$

VI. DISCUSSION

The analysis presented in this article focuses on a three-branch circuit identified by a charge and self-discharge cycle and highlights several aspects.

1) The uncertainty arising from the limited repeatability of the measurements influences parameters C_{i0} and C_{i1}, which largely describe the charging phase. In this case, the expanded uncertainty is $\leq$2%, $<$1.9%, and $<$0.3% for the 100-, 400-, and 1500-F SCs, respectively. The uncertainty of the measurement system has little weight in the charging phase: $<$0.2%, $<$0.2%, and $<$0.1% for the 100-, 400-, and 1500-F SCs, respectively.
2) The charging behavior is mainly influenced by parameters C_{i0} and C_{i1} but also changes due to the initial and the peak voltage drops on the ESR. The overall expanded uncertainties for parameter R_i are: $\leq$7%, $\leq$1.5%, and $\leq$1.2% for the 100-, 400-, and 1500-F SCs, respectively. The uncertainty of the measurement system is, also in this case, lower than the ones due to repeatability. Even though R_i overall uncertainty is higher than that of the other charging parameters, its terminal voltage sensitivity is significantly lower (see Figs. 4 and 5).
3) The self-discharge in the initial phase is largely governed by the parameters R_d and C_d, which extend their influence for minutes in smaller capacitors or tens of minutes in larger capacitors. In this case, the uncertainty in the determination of the parameters is $\leq$24%, $<$12%, and $\leq$3% for the 100-, 400-, and 1500-F SCs, respectively, whereas the instrumental uncertainty is $\leq$2.2%, $\leq$6%, and $\leq$1.4% for the three SCs. For these parameters, even a small bias (order of 1 mV) related to instrument uncertainty has a significant influence on the identification results. The positive outcome is that for these parameters the sensitivity with respect to the voltage at the terminals is reduced (see Fig. 5).
4) The effect of the bias is even more important in the identification of the parameters R_l and C_l. The uncertainty, term coming from the instrumentation, is of the same order of magnitude as the repeatability term, and even bigger for the 400-F SC. The overall uncertainty

of the two parameters R_l and C_l is $<15\%$ and $\leq 12\%$, respectively, for the 100-F SC, and $\leq 15\%$ and $<50\%$, respectively, for the 400-F SC. In this last case (400 F), the overall uncertainty mainly depends on the bias arising from the instrumental uncertainty and is possibly due to the incomplete charge of the capacitance C_l during the considered charging time.

VII. Conclusion

The SC capacitance is treated by manufacturers as a constant quantity, while it is a parameter depending on voltage. Moreover, the datasheet delivered by the manufacturers provides only a few data. As an example, at room temperature, for the 400-F SC Eaton declared a capacitance tolerance of -5% to $+10\%$, while SPS-CAP for the 1500 F declared a capacitance tolerance of -10% to $+20\%$. Apart from the series resistance, manufacturers do not provide the circuit parameters of the SC and provide just the capacitance, the energy/energy density of the SC, the nominal and maximum current values, the nominal voltage, the useful life cycles, and little else.

In other words, the data provided by manufacturers are fine for a rough sizing of storage systems but are not sufficient to implement SCs in complex applications.

As it is written in the introduction, the availability of SC equivalent circuits is useful for the modeling of SCs in complex electronic circuits often with batteries. SCs have to cope with fast charging and discharging phases [e.g., in electric vehicles during braking and accelerations, in PV panels, and in uninterruptible power supply (UPS)] and they must be controlled by systems, which drive the source or the load on the SC instead of the battery. These charge management systems (CMSs) are an extension of the battery management systems (BMSs), and in order to work properly, they need to control the SC using an ECM. The parameters of the ECM must be identified accurately, and the uncertainty of such parameters must be estimated.

This article provided a clear knowledge about parameters assessment and uncertainty estimation and provides guidance on how to go beyond the raw datasheet values to implement SCs in complex devices for applications, particularly in synergy with batteries.

Acknowledgment

The authors would like to thank the Horizon Europe programme and the European Partnership on Metrology for supporting this work in the framework of the projects Emphasis and MetSuperCap. Views and opinions expressed are however those of the author(s) only and do not necessarily reflect those of European Union or EURAMET (European Association of Metrology Institutes). Neither European Union nor the granting authority can be held responsible for them.

References

[1] S. Mašlán, "High capacitance simulation using mutual inductors," in *Proc. 24th IMEKO TC4 Int. Symp.*, Palermo, Italy, 2020, pp. 168–173.

[2] M. Catelani et al., "Experimental characterization of hybrid supercapacitor under different operating conditions using EIS measurements," *IEEE Trans. Instrum. Meas.*, vol. 73, pp. 1–10, 2024.

[3] M. Marracci, B. Tellini, M. Catelani, and L. Ciani, "Ultracapacitor degradation state diagnosis via electrochemical impedance spectroscopy," *IEEE Trans. Instrum. Meas.*, vol. 64, no. 7, pp. 1916–1921, Jul. 2015.

[4] G. Maria Lozito et al., "Equivalent circuit modelling of hybrid supercapacitors through experimental spectroscopic measurements," *IEEE Access*, vol. 12, pp. 78449–78462, 2024.

[5] J. Medved, A. Cultrera, M. Marzano, V. D'Elia, M. Ortolano, and L. Callegaro, "Traceable measurements of mutual inductance standards applied to large capacitance simulation in electrochemical impedance spectroscopy," in *Proc. Conf. Precis. Electromagn. Meas. (CPEM)*, Denver, CO, USA, Jul. 2024, pp. 1–2.

[6] *Fixed Electric Double-Layer Capacitors for Use in Electronic Equipment—Part 2: Sectional Specification—Electric Double Layer Capacitors for Power Application*, CEN-CENELEC B-1040, Standard EN 62391-2:2006, Brussels, Belgium, 2006.

[7] *Electric Double-Layer Capacitors for Use in Hybrid Electric Vehicles—Test Methods for Electrical Characteristics*, CEN-CENELEC, B-1040, Standard EN IEC 62576:2018, Brussels, Belgium, 2018.

[8] Z. Cabrane and S. H. Lee, "Electrical and mathematical modeling of supercapacitors: Comparison," *Energies*, vol. 15, no. 3, p. 693, Jan. 2022, doi: 10.3390/en15030693.

[9] F. Naseri, S. Karimi, E. Farjah, and E. Schaltz, "Supercapacitor management system: A comprehensive review of modeling, estimation, balancing, and protection techniques," *Renew. Sustain. Energy Rev.*, vol. 155, Mar. 2022, Art. no. 111913.

[10] Y. Chen, R. Yan, C. Yu, C. Zhao, X. Huang, and L. Wei, "Investigation on characteristic parameters identification and evolution of supercapacitor energy storage system from sparse and fragmented monitoring data," *IEEE Access*, vol. 11, pp. 56983–56993, 2023.

[11] A. Berrueta, A. Ursua, I. S. Martín, A. Eftekhari, and P. Sanchis, "Supercapacitors: Electrical characteristics, modeling, applications, and future trends," *IEEE Access*, vol. 7, pp. 50869–50896, 2019, doi: 10.1109/ACCESS.2019.2908558.

[12] H. Miniguano, A. Barrado, C. Fernández, P. Zumel, and A. Lázaro, "A general parameter identification procedure used for the comparative study of supercapacitors models," *Energies*, vol. 12, no. 9, p. 1776, May 2019.

[13] L. Zhang, X. Hu, Z. Wang, F. Sun, and D. G. Dorrell, "A review of supercapacitor modeling, estimation, and applications: A control/management perspective," *Renew. Sustain. Energy Rev.*, vol. 81, pp. 1868–1878, Jan. 2018, doi: 10.1016/j.rser.2017.05.283.

[14] Y. Parvini, J. B. Siegel, A. G. Stefanopoulou, and A. Vahidi, "Supercapacitor electrical and thermal modeling, identification, and validation for a wide range of temperature and power applications," *IEEE Trans. Ind. Electron.*, vol. 63, no. 3, pp. 1574–1585, Mar. 2016.

[15] M. Zucca, M. Hassanzadeh, O. Conti, and U. Pogliano, "Accurate parameters identification of a supercapacitor three-branch model," *IEEE Access*, vol. 11, pp. 122387–122398, 2023.

[16] M. Zucca, M. Hassanzadeh, D. Signorino, and U. Pogliano, "Measurement repeatability of a supercapacitor equivalent circuit parameters," in *Proc. Conf. Precis. Electromagn. Meas. (CPEM)*, Denver, CO, USA, Jul. 2024, pp. 1–2.

[17] R. Drummond, D. A. Howey, and S. R. Duncan, "Parameter estimation of an electrochemical supercapacitor model," in *Proc. Eur. Control Conf. (ECC)*, Aalborg, Denmark, Jun. 2016, pp. 1–6.

[18] R. Prasad, K. Kothari, and U. Mehta, "Flexible fractional supercapacitor model analyzed in time domain," *IEEE Access*, vol. 7, pp. 122626–122633, 2019.

[19] Q. Deng, D. Qiu, Z. Xie, B. Zhang, and Y. Chen, "Online SOC estimation of supercapacitor energy storage system based on fractional-order model," *IEEE Trans. Instrum. Meas.*, vol. 72, pp. 1–10, 2023.

[20] M. R. Kumar, S. Ghosh, and S. Das, "Analytical formulation for power, energy, and efficiency measurement of ultracapacitor using fractional calculus," *IEEE Trans. Instrum. Meas.*, vol. 68, no. 12, pp. 4834–4844, Dec. 2019.

[21] Y. Wang, G. Gao, X. Li, and Z. Chen, "A fractional-order model-based state estimation approach for lithium-ion battery and ultra-capacitor hybrid power source system considering load trajectory," *J. Power Sources*, vol. 449, Feb. 2020, Art. no. 227543.

[22] A. Dzieliński, G. Sarwas, and D. Sierociuk, "Comparison and validation of integer and fractional order ultracapacitor models," *Adv. Difference Equ.*, vol. 2011, p. 11, Jun. 2011.

[23] P. Mehra, S. Saxena, and S. Bhullar, "A comprehensive analysis of supercapacitors and their equivalent circuits—A review," *World Electr. Vehicle J.*, vol. 15, no. 8, p. 332, Jul. 2024, doi: 10.3390/wevj15080332.
[24] D. Slaifstein, F. M. Ibanez, and K. Siwek, "Supercapacitor modeling: A system identification approach," *IEEE Trans. Energy Convers.*, vol. 38, no. 1, pp. 192–202, Mar. 2023, doi: 10.1109/TEC.2022.3212617.
[25] P. Saha, S. Dey, and M. Khanra, "Modeling and state-of-charge estimation of supercapacitor considering leakage effect," *IEEE Trans. Ind. Electron.*, vol. 67, no. 1, pp. 350–357, Jan. 2020.
[26] L. E. Helseth, "Modelling supercapacitors using a dynamic equivalent circuit with a distribution of relaxation times," *J. Energy Storage*, vol. 25, Oct. 2019, Art. no. 100912.
[27] M. Ates and A. Chebil, "Supercapacitor and battery performances of multi-component nanocomposites: Real circuit and equivalent circuit model analysis," *J. Energy Storage*, vol. 53, Sep. 2022, Art. no. 105093.
[28] S. Buller, E. Karden, D. Kok, and R. W. De Doncker, "Modeling the dynamic behavior of supercapacitors using impedance spectroscopy," *IEEE Trans. Ind. Appl.*, vol. 38, no. 6, pp. 1622–1626, Nov. 2002.
[29] G. J. Adekoya, O. C. Adekoya, U. K. Ugo, E. R. Sadiku, Y. Hamam, and S. S. Ray, "A mini-review of artificial intelligence techniques for predicting the performance of supercapacitors," *Mater. Today: Proc.*, vol. 62, no. 1, pp. S184–S188, 2022, doi: 10.1016/j.matpr.2022.05.079.
[30] A. R. Conn, N. I. M. Gould, and P. L. Toint, "Trust region methods," in *MOSSIAM Series on Optimization*. Philadelphia, PA, USA: SIAM, 2000.
[31] R. Prasad, U. Mehta, K. Kothari, M. Cirrincione, and A. Mohammadi, "Supercapacitor parameter identification using grey wolf optimization and its comparison to conventional trust region reflection optimization," in *Proc. Int. Aegean Conf. Elect. Mach. Power Electron. (ACEMP) Int. Conf. Optim. Elect. Electron. Equip. (OPTIM)*, Istanbul, Turkey, 2019, pp. 563–569, doi: 10.1109/ACEMP-OPTIM44294.2019.9007158.
[32] M. L. Johnson and L. M. Faunt, "Parameter estimation by least-squares methods," *Methods in Enzymology*, vol. 210. New York, NY, USA: Academic, 1992, pp. 1–37.

Mauro Zucca (Senior Member, IEEE) received the Ph.D. degree in electrical engineering from the Politecnico di Torino, Turin, Italy, in 1998.

In 2012, he achieved the qualification as Associate Professor of electrical engineering. Since 2017, he has been a Senior Researcher. He is currently a Chief at the "Electromagnetic Fields and Systems" Group at Istituto Nazionale di Ricerca Metrologica (INRiM), Turin. His articles have more than 1100 citations (H_index 21). He participated in over 100 conferences, ten of which by invitation, and is the author of over 90 publications in international peer-reviewed journals. He was responsible for eight research contracts and participated in 16 collaborative research projects: in four of them as a Principal Investigator. He is the co-author of three patents and commercial software for computational electromagnetics. His activity includes the study and design of electromagnetic devices, storage, shielding of power systems, and inductive charging.

Dr. Zucca is a member of the Technical Committee TC106 of the Italian Electrotechnical Committee (CEI).

Melika Hassanzadeh received the B.S. and M.Sc. degrees in electrical engineering from the Babol Noshirvani University of Technology, Babol, Iran, in 2011 and 2014, respectively. She is currently pursuing the Ph.D. degree in metrology with the Politecnico di Torino, Turin, Italy.

She is performing her research activity with Istituto Nazionale di Ricerca Metrologica (INRiM), Turin. She is currently participating in two EU research projects, *Emphasis* and *MetSuperCap*, that deal with supercapacitors (SCs). Her research interests include the modeling of supercapacitors, and she has experience both in modeling and software development and in laboratory practice, including signal generation, conditioning, and acquisition.

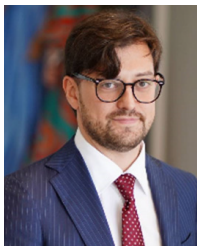

Davide Signorino was born in Naples, Italy, in 1990. He received the Ph.D. degree in metrology from the Politecnico di Torino, Turin, Italy, in 2022.

He is currently a Permanent Researcher at the Italian National Metrology Institute (INRiM), Turin. His research focuses on metrology applied to transportation systems, particularly analyzing energy flow between the supply line and trains, calibrating energy meters, and characterizing voltage and current transducers under static and dynamic conditions. In addition, he contributes to research on power quality in dc systems.

Umberto Pogliano was born in Turin, Italy, in 1950. He received the Dr.Ing. degree in electronic engineering and the Ph.D. degree in metrology from the Politecnico di Torino, Turin, in 1975 and 1987, respectively.

In 1977, he joined the Electrical Metrology Department, Istituto Nazionale di Ricerca Metrologica (INRiM), Turin, where his research focused on the development of systems and procedures for precise dc and ac low-frequency measurements. His main interests include ac–dc transfer standard, ac voltage, current, power measurements, generation, acquisition, and reconstruction of electrical signals. Since 2015, he has retired but still cooperates as a metrology expert in some INRiM projects and activities.